INTERNATIONAL JOURNAL FOR NUMERICAL METHODS IN FLUIDS, VOL. 24, 1–15 (1997)

NUMERICAL SIMULATION OF SHALLOW WATER WAVE PROPAGATION USING A BOUNDARY ELEMENT WAVE EQUATION MODEL

N. BENMANSOUR AND D. OUAZAR

Ecole Mohammadia d'Ingenieurs, LASH, BP 765 Agdal, Rabat, Morocco

AND

L. C. WROBEL

Brunel University, Department of Mechanical Engineering, Uxbridge, Middlesex UB8 3PH, UK

SUMMARY

The present paper makes use of a wave equation formulation of the primitive shallow water equations to simulate one-dimensional free surface flow. A numerical formulation of the boundary element method is then developed to solve the wave continuity equation using a time-dependent fundamental solution, while an explicit finite difference scheme is used to derive velocities from the primitive momentum equation. One-dimensional free surface flows in open channels are treated and the results compared with analytical and numerical solutions.

KEY WORDS: shallow water equations; boundary element method; wave equation model; free surface flow

1. INTRODUCTION

One of the most interesting areas of application of numerical methods in hydraulics is the simulation of free surface flow in shallow waters. The equations describing this type of flow are obtained by integrating the Navier-Stokes equations for conservation of mass and momentum through the vertical column of fluid.

Several of the early finite element tidal models based on the primitive shallow water equations were plagued by spurious spatial oscillations. Field-scale simulations invariably required artificial viscosity or numerical damping to achieve stable solutions.[1,2]

A successful approach to eliminate these node-to-node oscillations was developed by Lynch and Gray.[3] This approach, called the wave equation model, is based on a reformulation of the primitive continuity equation into a second-order wave continuity form. Because of the advantageous numerical properties, the approach received considerable attention for finite element tidal computations.

Although the boundary element method (BEM) has proven to be a powerful alternative for solution of wave propagation problems,[4,5] its application to hyperbolic-type equations is still limited, especially in the presence of non-linearities. A formulation of the BEM for one-dimensional wave propagation problems was presented by Benmansour *et al*.[6] Using the fundamental solution of the

CCC 0271–2091/97/010001–15

Received December 1995

wave operator, an integral equation was obtained after some necessary transformations to evaluate integrals involving Heaviside and Dirac delta functions. The BEM formulation was then employed to analyse simple problems of free surface flow in open rectangular channels[7] in which convective effects were neglected.

In the present paper the BEM formulation of the one-dimensional wave continuity equation is extended to include non-linear effects. The non-homogeneous part of this equation is treated as a known term by using values obtained from the previous time step. An iteration procedure is necessary, however, because of the presence of non-linear effects. The formulation uses a finite difference scheme to solve the momentum equation.

Finally, several applications are presented to highlight some of the potentialities of this approach in solving free surface flow in open channels.

2. GOVERNING EQUATIONS

2.1. Primitive shallow water equations

The shallow water equations describing the one-dimensional free surface flow in a rectangular channel are obtained by integrating the equations for conservation of mass and momentum through the vertical column of fluid under the following assumptions:

1. The density of the fluid is constant.
2. The viscosity term is negligible.
3. The vertical fluid accelerations are negligible.

The following set of coupled equations is then obtained:

continuity equation

$$L = \frac{\partial h}{\partial t} + \frac{\partial (hu)}{\partial x} = 0, \tag{1}$$

momentum equation

$$M = \frac{\partial u}{\partial t} + u\frac{\partial u}{\partial x} + g\frac{\partial \eta}{\partial x} + \tau u = 0, \tag{2}$$

where h is the total fluid depth, u is the velocity, g is the gravitational acceleration, η is the free surface elevation and τ is the bottom friction parameter.

The momentum equation can also be formulated in conservative form as

$$M^{\mathrm{c}} = hM + uL = 0$$

or in expanded form as

$$\frac{\partial (hu)}{\partial t} + \frac{\partial (huu)}{\partial x} + gh\frac{\partial \eta}{\partial x} + \tau hu = 0. \tag{3}$$

2.2. Wave equation formulation

The wave equation formulation of the primitive shallow water equations was first introduced by Lynch and Gray.[3] This approach is based on a reformulation of the continuity equation into a second-order in time and space propagation form.

The wave equation form can be written in operator notation as[3]

$$\frac{\partial L}{\partial t}-\frac{\partial M^{c}}{\partial x}+\tau L=0, \tag{4}$$

in which L and M are the continuity and momentum operators respectively. The solution of equation (4) in conjunction with (2) will lead to the same solution of (1) and (2) under the condition that $L=0$ at $t=0$.[8] For the BEM formulation the additional initial condition is equivalent to the specification of $\partial\eta/\partial t$ at $t=0$.

Substitution of the continuity and momentum operators in equation (4) leads to

$$\frac{\partial^2 h}{\partial t^2}=g\frac{\partial}{\partial x}\left(h\frac{\partial\eta}{\partial x}\right)+\frac{\partial^2(huu)}{\partial x^2}-\tau\frac{\partial h}{\partial t}+hu\frac{\partial\tau}{\partial x}. \tag{5}$$

Let $h=H-h_{\mathrm{b}}+\eta$, in which H is the average depth and h_{b} is the bottom variation, both measured from a reference datum (Figure 1). Equation (5) then becomes

$$\frac{\partial^2\eta}{\partial t^2}-c^2\frac{\partial^2\eta}{\partial x^2}=g\frac{\partial}{\partial x}\left(\eta\frac{\partial\eta}{\partial x}\right)-g\frac{\partial}{\partial x}\left(h_{\mathrm{b}}\frac{\partial\eta}{\partial x}\right)+\frac{\partial^2(huu)}{\partial x^2}-\tau\frac{\partial\eta}{\partial t}+hu\frac{\partial\tau}{\partial x}, \tag{6}$$

in which $c=\sqrt{(gH)}$ is the wave celerity.

For the numerical solution with the BEM the above equation will be treated as a non-homogeneous wave equation with a known right-hand side term which is a function of several variables, in the form

$$\frac{\partial^2\eta}{\partial t^2}-c^2\frac{\partial^2\eta}{\partial x^2}=B\left(\frac{\partial\eta}{\partial x},\frac{\partial\eta}{\partial t},u,h,\ldots\right). \tag{7}$$

3. BEM FORMULATION

The BEM formulation proposed in this paper consists of using the fundamental solution of the wave equation and treating the non-homogeneous term B as known by evaluating it using values calculated at the previous time step. This procedure is particularly efficient when the wave equation can be linearized and uncoupled from the momentum equation.

The starting weighted residual statement corresponding to equation (7) can be written as

$$\int_0^{t_F^+}\int_0^L\left(\frac{\partial^2\eta}{\partial t^2}-c^2\frac{\partial^2\eta}{\partial x^2}\right)\eta^*\mathrm{d}x\mathrm{d}t=\int_0^{t_F^+}\int_0^L B\eta^*\mathrm{d}x\mathrm{d}t, \tag{8}$$

where L is the region length and $t_F^+=t_F+\epsilon$, ϵ being a small arbitrary parameter. This procedure avoids terminating the integrations exactly at the peak of a Dirac delta function.[9]

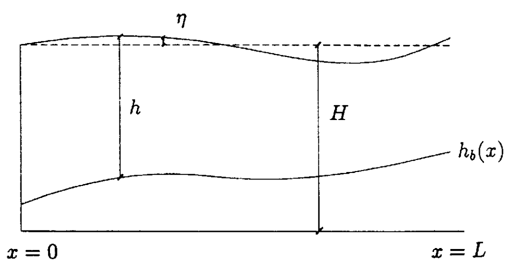

Figure 1. Sketch of one-dimensional open channel flow

In the above expression η^* is the fundamental solution of the one-dimensional wave operator, given by

$$\eta^* = -\frac{1}{2c} H[c(t_F - t) - r],$$

in which H is the Heaviside function and $r = |x - s|$, s and x indicating the source and field point positions respectively.

Integrating the second-order derivatives in (8) twice by parts, the following equation is obtained:

$$\int_0^{t_F^+}\int_0^L \left(\frac{\partial^2 \eta^*}{\partial t^2} - c^2 \frac{\partial^2 \eta^*}{\partial x^2}\right)\eta \mathrm{d}x\mathrm{d}t + \int_0^L \left[\eta^* \frac{\partial \eta}{\partial t} - \eta \frac{\partial \eta^*}{\partial t}\right]_0^{t_F^+} \mathrm{d}x - c^2 \int_0^{t_F^+} \left[\eta^* \frac{\partial \eta}{\partial x} - \eta \frac{\partial \eta^*}{\partial x}\right]_0^L \mathrm{d}t = \int_0^{t_F^+}\int_0^L B\eta^* \mathrm{d}x\mathrm{d}t. \tag{9}$$

The causality property of the Heaviside function,[9] i.e.

$$H[c(t_F - t) - r] = 0 \quad \text{if} \quad c(t_F - t) < r,$$

leads to

$$\eta^*|^{t_F+\epsilon} = 0 \quad \text{and} \quad \frac{\partial \eta^*}{\partial t}|^{t_F+\epsilon} = 0.$$

The following integral equation is then obtained:

$$\eta(s, t_F) = c^2 \int_0^{t_F} \left[\eta \frac{\partial \eta^*}{\partial x} - \eta^* \frac{\partial \eta}{\partial x}\right]_0^L \mathrm{d}t + \int_0^L \left[\eta \frac{\partial \eta^*}{\partial t} - \eta^* \frac{\partial \eta}{\partial t}\right]_{t=0} \mathrm{d}x - \int_0^{t_F}\int_0^L B\eta^* \mathrm{d}x\mathrm{d}t. \tag{10}$$

Noticing that the fundamental solution η^* can be written in the form

$$\eta^* = \begin{cases} -\dfrac{1}{2c} H[x - (s - c(t_F - t))] & \text{if} \quad x < s, \\ -\dfrac{1}{2c}\{1 - H[x - (s + c(t_F - t))]\} & \text{if} \quad x > s, \end{cases}$$

the properties of the Heaviside and Dirac delta functions can be used to evaluate the derivatives of η^* with respect to time and space as follows:

$$\begin{aligned}\frac{\partial \eta^*}{\partial t} &= -\frac{1}{2c}\frac{\partial}{\partial t} H[-ct + ct_F - r] = -\frac{1}{2c}\frac{\partial}{\partial t}\{1 - H[ct - (ct_F - r)]\} \\ &= \tfrac{1}{2}\delta[c(t - t_F) + r] = \tfrac{1}{2}\delta[c(t_F - t) - r],\end{aligned}$$

$$\frac{\partial \eta^*}{\partial x} = \begin{cases} -\dfrac{1}{2c}\delta[x - (s - c(t_F - t))] & \text{if} \quad x < s, \\ \dfrac{1}{2c}\delta[x - (s + c(t_F - t))] & \text{if} \quad x > s. \end{cases}$$

Using the above expressions to evaluate the integrals in equation (10) and assuming $\eta(x, 0)$ and $(\partial\eta/\partial t)(x, 0)$ as known initial conditions, equation (10) becomes[10]

$$\begin{aligned}\eta(s, t_F) = &\tfrac{1}{2}[\eta(L, t_F - (L - s)/c) + \eta(0, t_F - s/c] + \frac{c}{2}\left(\int_0^{t_F-(L-s)/c} \frac{\partial \eta}{\partial x}(L, t)\mathrm{d}t - \int_0^{t_F - s/c} \frac{\partial \eta}{\partial x}(0, t)\mathrm{d}t\right) \\ &+ \tfrac{1}{2}[\eta(s - ct_F, 0) + \eta(s + ct_F, 0)] + \frac{1}{2c}\int_{s-ct_F}^{s+ct_F} \frac{\partial \eta}{\partial t}(x, 0)\mathrm{d}x - \int_0^{t_F}\int_0^L B\eta^* \mathrm{d}x\mathrm{d}t.\end{aligned} \tag{11}$$

The terms involved in the above expression are only valid when all arguments are physically meaningful. Hence time and space co-ordinates must be within the domain of interest, i.e. $[0, L] \times [0, t_F]$, and the integrals must have their lower bound smaller than the upper one, otherwise they are equal to zero.

Singularities occurring in the integrals involving the Dirac delta function at points $s = ct_F$ or $L - ct_F$ are avoided by using an appropriate transformation of the function η at these points.[10]

3.1. Computation of domain integral

For the numerical computation of the domain integral the segment $[0, L]$ is discretized into M elements and the time dimension is subdivided into F time steps. The non-homogeneous term B is then assumed to vary within each element and each time step according to space and time interpolation functions such that

$$B(x, t) = \sum_{j=0}^{F-1} \sum_{i=0}^{M-1} \phi^j(t)\psi_i(x)B_i^j,$$

where $B_i^j = B(x_i, t_j)$.

The domain integral

$$D = \int_0^{t_F} \int_0^L B\eta^* \mathrm{d}x\mathrm{d}t \tag{12}$$

becomes, after discretization,

$$D = \sum_{j=0}^{F-1} \sum_{i=0}^{M-1} B_i^j D_{ij}, \tag{13}$$

with

$$D_{ij} = \int_0^{t_F} \int_0^L \phi^j(t)\psi_i(x)\eta^* \mathrm{d}x\mathrm{d}t.$$

In this work both constant and linear interpolation functions are tested.

If constant time interpolation functions are used, the body force term B is treated as a known term by using values obtained from the previous time step. In this case $\phi^j(t)$ is defined in the form

$$\phi^j(t) = \begin{cases} 1 & \text{if} \quad t_j \leqslant t < t_{j+1}, \\ 0 & \text{otherwise} \quad . \end{cases}$$

The integral D_{ij} then becomes

$$D_{ij} = -\frac{1}{2c} \int_{t_j}^{t_{j+1}} \int_0^L \psi_i(x) H[c(t_F - t) - r] \mathrm{d}x\mathrm{d}t. \tag{14}$$

The above procedure is simple and particularly efficient for linear problems. However, if non-linear effects are important, an iterative technique is required for the solution of the system of equations. In this case much improved results may be obtained by using linear time interpolation functions.

The accuracy of the results can also be improved by keeping constant time interpolation functions and using the mean value of B in the time interval such that

$$B^j(x) = \begin{cases} \frac{1}{2}[B(x, t_j) + B(x, t_{j+1})] & \text{if} \quad t_j \leqslant t < t_{j+1} \quad \text{and} \quad j < F - 1, \\ B(x, t_j) & \text{if} \quad t_j \leqslant t < t_{j+1} \quad \text{and} \quad j = F - 1. \end{cases}$$

For constant space interpolation functions, $\psi_i(x)$ is defined in the form

$$\psi_i(x) = \begin{cases} 1 & \text{if} \quad x_i \leqslant x < x_{i+1}, \\ 0 & \text{otherwise.} \end{cases}$$

The integral (14) then reduces to

$$D_{ij} = -\frac{1}{2c}\int_{t_j}^{t_{j+1}}\int_{x_i}^{x_{i+1}} H[c(t_F - t) - r]\mathrm{d}x\mathrm{d}t,$$

which can be evaluated analytically as described in Reference 10.

For linear space interpolation functions, in which case $\psi_i(x)$ is defined in the form

$$\psi_i(x) = \begin{cases} \dfrac{x - x_{i-1}}{x_i - x_{i-1}} & \text{if} \quad x_{i-1} < x \leqslant x_i, \\ \dfrac{x_{i+1} - x}{x_{i+1} - x_i} & \text{if} \quad x_i \leqslant x < x_{i+1}, \\ 0 & \text{otherwise,} \end{cases}$$

the integral (14) may be simplified by using the causality property of the Heaviside function:

$$D_{ij} = -\frac{1}{2c}\int_{t_j}^{t_{j+1}}\int_{X_1(t)}^{X_2(t)} \psi_i(x)\mathrm{d}x\mathrm{d}t, \tag{15}$$

where $X_1(t) = s - c(t_F - t)$ and $X_2(t) = s + c(t_F - t)$. The integral (15) can then be written as

$$D_{ij} = -\frac{1}{2c}\int_{t_j}^{t_{j+1}} F(t)\mathrm{d}t,$$

where

$$F(t) = \int_{X_1(t)}^{X_2(t)} \psi_i(x)\mathrm{d}x.$$

The integrals in this case are evaluated numerically using standard Gaussian quadrature for the function $F(t)$.

Simple finite difference schemes are used to calculate first- and second-order derivatives that appear in the term B (see equation (6)). The following expressions are employed for the space derivatives at point i, $1 < i < M$:

$$\left[\frac{\partial\eta}{\partial x}\right]_i^j = \frac{\eta_{i+1}^j - \eta_{i-1}^j}{2\Delta x}$$

$$\left[\frac{\partial^2(huu)}{\partial x^2}\right]_i^j = \frac{(huu)_{i+1}^j - 2(huu)_i^j + (huu)_{i-1}^j}{(\Delta x)^2}.$$

At the end points,

$$\left[\frac{\partial\eta}{\partial x}\right]_1^j = \frac{-3\eta_1^j + 4\eta_2^j - \eta_3^j}{2\Delta x},$$

$$\left[\frac{\partial^2(huu)}{\partial x^2}\right]_1^j = \frac{2(huu)_1^j - 5(huu)_2^j + 4(huu)_3^j - (huu)_4^j}{(\Delta x)^2}$$

$$\left[\frac{\partial\eta}{\partial x}\right]_M^j = \frac{3\eta_M{}^j - 4\eta_{M-1}^j + \eta_{M-2}^j}{2\Delta x},$$

$$\left[\frac{\partial^2(huu)}{\partial x^2}\right]_M^j = \frac{2(huu)_M^j - 5(huu)_{M-1}^j + 4(huu)_{M-2}^j - (huu)_{M-3}^j}{(\Delta x)^2}.$$

A second-order finite difference approximation is also used to compute the time derivative in the form

$$\left[\frac{\partial\eta}{\partial t}\right]_i^j = \begin{cases} \dfrac{3\eta_i^j - 4\eta_i^{j-1} + \eta_i^{j-2}}{2\Delta t} & \text{for} \quad j \geq 3, \\ \dfrac{\eta_i^j - \eta_i^{j-1}}{\Delta t} & \text{for} \quad j = 2 \end{cases}.$$

3.2. Finite difference solution of momentum equation

Although the solution of the wave equation is accurately obtained by the boundary element formulation, the numerical representation of the momentum equation is very important in determining the evolution of the numerical simulation.

Kinnmark and Gray[11] showed the importance of a proper time weighting in the discretization of the momentum equation. Using Fourier analysis, they concluded that a three-time-level scheme, especially when centred in time, can result in step-by-step temporal oscillations in the velocity solution, although similar oscillations in the surface elevation are eliminated by the wave equation. By using a two-time-level scheme for the time derivatives, spurious $2\Delta t$ oscillations were completely removed from the velocity solution. These findings were subsequently confirmed by Foreman[12] and Laible.[13]

Consequently, a simple differencing scheme of the momentum equation between time levels F and $F-1$ is used for the velocity calculations. Each term in the momentum equation (2) is approximated as follows:

$$\left[\frac{\partial u}{\partial t}\right]_i^F = \frac{u_i^F - u_i^{F-1}}{\Delta t},$$

$$\left[\frac{\partial\eta}{\partial x}\right]_i^F = \alpha\left[\frac{\partial\eta}{\partial x}\right]_i^F + (1-\alpha)\left[\frac{\partial\eta}{\partial x}\right]_i^{F-1},$$

$$u_i^F = \theta u_i^F + (1-\theta)u_i^{F-1},$$

$$\left[u\frac{\partial u}{\partial x}\right]_i^F = \Psi\left[u\frac{\partial u}{\partial x}\right]_i^F + (1-\Psi)\left[u\frac{\partial u}{\partial x}\right]_i^{F-1},$$

in which θ, α and Ψ are time-weighting parameters.

Replacing each term by its finite difference approximation, the momentum equation (2) may be written in the form

$$u_i^F(1+\theta\Delta t\tau_i^{F-1}) = u_i^{F-1} - \Delta t\left(\Psi u_i^F\left[\frac{\partial u}{\partial x}\right]_i^F + (1-\Psi)u_i^{F-1}\left[\frac{\partial u}{\partial x}\right]_i^{F-1} + g\alpha\left[\frac{\partial \eta}{\partial x}\right]_i^F + g(1-\alpha)\left[\frac{\partial \eta}{\partial x}\right]_i^{F-1} + \tau_i^{F-1}(1-\theta)u_i^{F-1}\right). \tag{16}$$

4. SOLUTION PROCEDURE

The general solution procedure consists of solving the wave continuity equation for the elevation η using a boundary element formulation, while the velocities are derived from the primitive momentum equation by a finite difference technique. At each time step these equations are solved sequentially rather than simultaneously. For this the domain term B in the BEM analysis is evaluated using values from the previous time step.

The above procedure is particularly efficient in that no iterations are required for equations involving mild non-linearities. In this case the term B can be accurately computed and the convective terms in the momentum equation may be evaluated explicitly.

On the other hand, if convective effects are important and the surface elevation η is not negligible in comparison with the total water depth, an iterative technique is required, as described next.

4.1. Iterative technique

For non-linear problems the following iterative procedure is employed at each time t_F:

1. With known values of velocity and elevation from the previous time step, calculate the domain integral at each boundary and internal point.
2. The wave equation is used to evaluate either η or $\partial\eta/\partial x$ at boundary points.
3. The wave equation is used to evaluate values of η at all internal points.
4. The momentum equation is used to compute values of the velocity at boundary and internal points. The convective term is evaluated explicitly by setting the value of Ψ to zero.
5. Using values of η and u at the new time level, the term B is recomputed. The domain integrals are now evaluated considering a mean value of B in the interval $[t_F - \Delta t, t_F]$.
6. The wave equation is again applied to compute updated values of η at boundary and internal points.
7. The momentum equation is again applied to compute values of the velocity by considering an implicit approximation of all the terms in the equation.
8. The convergence of η and u is examined at all boundary and internal points. Unless convergence is achieved, the procedure is repeated from step 5 with the updated values of η and u.

Since the initial values of η and u are those from the previous time step, only one or two iterations are usually necessary even for highly non-linear problems.

5. APPLICATIONS

In order to verify the accuracy and efficiency of the numerical scheme previously developed, the model is applied to the study of free surface flow in open rectangular channels. Initially the model was applied to some standard test cases with known analytical solutions.[14] Although such solutions are only available for linear problems, they are a valuable tool for assessing various aspects of the performance of the numerical model.

The model was next applied to study the effect of non-linear forcing terms for two problems. The first consists of the propagation of a wave front in a horizontal channel and is usually considered as an extreme test situation for numerical methods.[15] The second case deals with the routing of a flood wave down a rectangular channel[16] and provides a good test for the iterative procedure developed here.

5.1. Linear problems

The first series of tests deals with long waves propagating in open channels with the following configurations:

(a) constant depth and no bottom friction
(b) constant depth and linearized bottom friction
(c) quadratic bottom variation and no friction
(d) quadratic bottom variation and linearized friction.

In all cases the channel is closed at one end and subject to a sinusoidal forcing at the other end where the water level is prescribed as a boundary condition. Analytical solutions have been presented by Lynch and Gray[14] assuming that convective terms are neglected and $(\partial\eta/\partial x)^2 \approx 0$.

5.1.1. Channel with constant depth. The first application is a simple rectangular channel of length $L = 160$ m and constant depth $H = 2$ m, subject to an incident wave of amplitude $\eta_0 = 0{\cdot}1$ m and period $T = 200$ s prescribed at the open end, as shown in Figure 2.

The analytical solution is given by[14]

$$\eta(x, t) = \mathrm{Re}\left(\eta_0 \frac{\cos[\beta(x - x_1)]}{\cos(\beta L)} \mathrm{e}^{\mathrm{i}\omega t}\right), \qquad u(x, t) = \mathrm{Re}\left(-\frac{\mathrm{i}\omega\eta_0}{\beta H} \frac{\sin[\beta(x - x_1)]}{\cos(\beta L)} \mathrm{e}^{\mathrm{i}\omega t}\right),$$

where $\omega = 2\pi/T$, $L = x_2 - x_1$ and $\beta^2 = (\omega^2 - \mathrm{i}\omega\tau)/gH$.

Two different values of the linearized bottom friction coefficient τ are considered:

(a) $\tau = 0$, i.e. the case of no bottom friction
(b) $\tau = 0{\cdot}01$ s^{-1}.

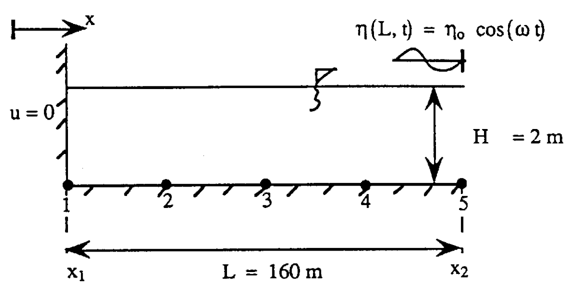

Figure 2. Rectangular open channel of constant depth

For the first case the forcing term B vanishes and no domain discretization is necessary. Thus the BEM solution of the wave equation produces a system of two equations for η at $x=0$ and $\partial\eta/\partial x$ at $x=L$. After solution of this system, values of η at internal points can be calculated if required.

This is a very simple case which provides little indication as to the ability of the model to simulate real cases involving complex geometries or non-linear effects. However, this test can provide guidelines for the choice of the value of the Courant number and other parameters used in the numerical procedure.

Table I compares numerical and analytical results for η at $x=0$ and $L/2$. It can be seen that the numerical results exactly match the analytical solution, since space and time integrations need not be performed in this particular case. A time step $\Delta t=9$ s was used in the analysis.

Table II shows results for the velocity at point $x=L$ obtained by the finite difference scheme with a discretization of four segments, i.e. $\Delta x=L/4$, for three different values of the Courant number $Cr=c\Delta t/\Delta x$. Since the depth is constant and η is small compared with h, then $H=h$ and the wave celerity is given by $c=\sqrt{(gH)}=4{\cdot}429$ m s^{-1}. The time-weighting parameter α was taken as 0·5. It can be seen that, as expected, better results are obtained for $Cr \leqslant 1{\cdot}0$.

Next bottom friction effects were considered by setting $\tau=0{\cdot}01$ s^{-1}. In this case the BEM formulation presents a domain integral with $B=-\tau(\partial\eta/\partial t)$. To compute this term, a discretization with $\Delta x=L/4$ was introduced and the elevations at points $x=0$ and $L/2$ are plotted in Figure 3. Excellent agreement between numerical results obtained with $Cr=1{\cdot}0$ and the analytical solution can be noticed.

Figure 4 shows results for the water velocity at two different points of the channel, $x=L/2$ and L. Several different combinations of parameters α and θ were tested: their optimal values were found to lie between 0·5 and 0·7 for α and between 0·3 and 0·7 for θ. The results in Figure 4 were obtained using both α and θ equal to 0·5.

Table I. Elevation results (metres) for $\tau=0$

	$x=0$		$x=L/2$	
t (s)	BEM	Analytical	BEM	Analytical
27	0·155	0·155	0·131	0·131
81	−0·194	−0·194	−0·164	−0·164
162	0·086	0·086	0·073	0·073
270	−0·138	−0·138	−0·116	−0·116
378	0·181	0·181	0·152	0·152

Table II. Velocity results (metres per second) for $\tau=0$ at point $x=L$

	FDM			
t (s)	$Cr=0{\cdot}5$	$Cr=1{\cdot}0$	$Cr=1{\cdot}5$	Analytical
27	0·354	0·354	0·354	0·354
40·5	0·446		0·439	0·451
81	0·265	0·265	0·261	0·265
121·5	−0·290		−0·270	−0·295
162	−0·439	−0·439	−0·431	−0·439
229·5	0·381		0·352	0·377
270	0·382	0·382	0·398	0·382
378	−0·301	−0·301	−0·320	−0·301

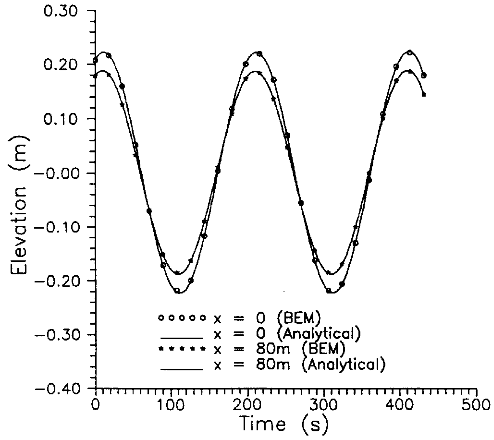

Figure 3. BEM elevation results for channel with constant depth, $\tau = 0{\cdot}01\ \mathrm{s}^{-1}$

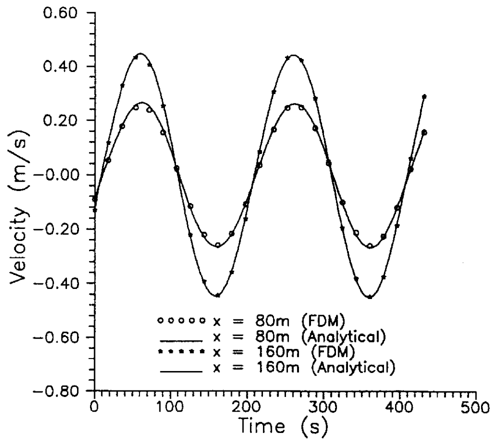

Figure 4. FDM velocity results for channel with constant depth, $\tau = 0{\cdot}01\ \mathrm{s}^{-1}$

5.1.2. Channel with quadratic bottom variation. This application concerns a channel with quadratic bottom variation, with water depth 1 m at the closed end and 2 m at the open end, subject to the same sinusoidal wave as in Figure 2.

The analytical solution for this case is[14]

$$\eta(x,t) = \mathrm{Re}[(Ax^{s_1} + Bx^{s_2})\mathrm{e}^{\mathrm{i}\omega t}], \qquad u(x,t) = \mathrm{Re}\left(\frac{\mathrm{i}\omega}{\beta^2 H_0}(As_1 x^{s_1-1} + Bs_2 x^{s_2-1})\mathrm{e}^{\mathrm{i}\omega t}\right),$$

where

$$A = \frac{\eta_0 s_2 x_1^{s_2}}{s_2 x_1^{s_2} x_2^{s_1} - s_1 x_1^{s_1} x_2^{s_2}}, \qquad B = \frac{-\eta_0 s_1 x_1^{s_1}}{s_2 x_1^{s_2} x_2^{s_1} - s_1 x_1^{s_1} x_2^{s_2}},$$

$$s_1, s_2 = -\tfrac{1}{2} \pm \sqrt{(\tfrac{1}{4} - \beta^2)}, \qquad H(x) = H_0 x^2, \qquad \beta^2 = \frac{\omega^2 - \mathrm{i}\omega\tau}{gH_0}.$$

The analysis takes into consideration the channel reach between points $x_1 = 386{\cdot}274$ m and $x_2 = 546{\cdot}274$ m with water depths 1 and 2 m respectively. These values of x_1 and x_2 are used in the analytical solution, together with $H_0 = 6{\cdot}702 \times 10^{-6}\ \mathrm{m}^{-1}$. For the numerical solution the channel end points are at $x = 0$ and $x = L = 160$ m, with $h_\mathrm{b} = 1 - x^2/25{,}600$ m. The celerity used in the computations is $c = \sqrt{(gH)}$, where $H = 2$ m.

Again the same values of the linearized bottom friction coefficient τ are considered, i.e. $\tau = 0$ and $0{\cdot}01\ \mathrm{s}^{-1}$. The discretization adopted employed only four segments, i.e. $\Delta x = 40$ m and $\Delta t = 9$ s, giving a Courant number $Cr = 1$.

For the case of $\tau = 0$ the forcing term B in equation (7) is a function of $h_\mathrm{b}\partial\eta/\partial x$ only. BEM results for the elevation and FDM results for the velocity are shown in Figures 5 and 6 respectively, compared with the analytical solution. The agreement is excellent in both cases.

Finally the case of $\tau = 0{\cdot}01\ \mathrm{s}^{-1}$ was considered. Thus both linear domain terms in equation (7) are simultaneously included. Again excellent results are obtained from the numerical analysis, as shown in Figures 7 and 8. The velocity results were obtained with both α and θ equal to 0·5.

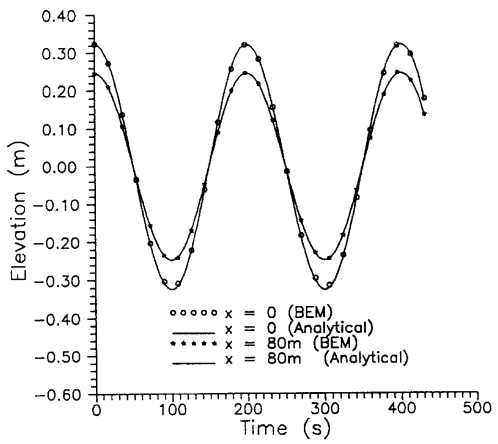

Figure 5. BEM elevation results for channel with quadratic bottom variation, $\tau = 0$

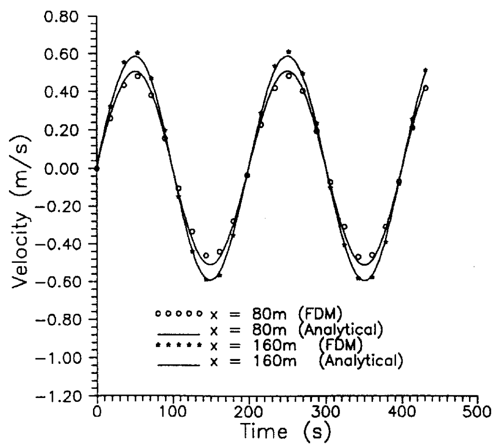

Figure 6. FDM velocity results for channel with quadratic bottom variation, $\tau = 0$

5.2. Propagation of a wave front in a frictionless channel

This test, described in Reference 15, consists of the propagation of a wave front in a horizontal, frictionless channel 5000 m long. The channel is open at the left boundary, where the water level is suddenly raised from the initial state of rest of 10 m to 10·1 m within one time step (see Figure 9). At the right end the channel is closed and the velocity is set to zero.

This problem is considered to be an extreme test situation for numerical models, as the exact solution is a step function for the state variables. However, this situation is accurately and efficiently reproduced by the BEM, since the numerical solution procedure for the wave equation is itself based on the Heaviside step function. Therefore, by using the boundary integral expression (11) and applying the initial and boundary conditions of this particular case, the exact solution for η at any point s along the channel is found in the form

$$\eta(s, t_F) = \eta(0, t_F - s/c) + \tfrac{1}{2}[\eta(L, t_F - a + s/c) - \eta(L, t_F - a - s/c)],$$

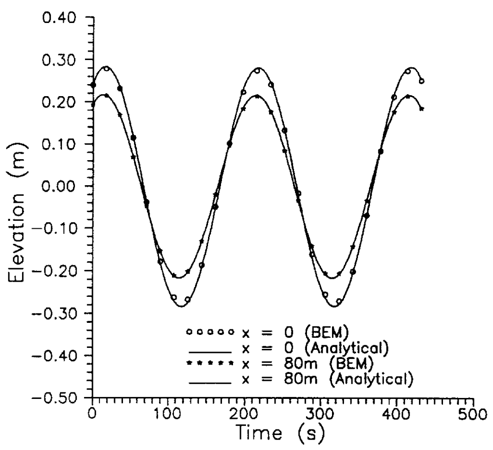

Figure 7. BEM elevation results for channel with quadratic bottom variation, $\tau = 0{\cdot}01\ s^{-1}$

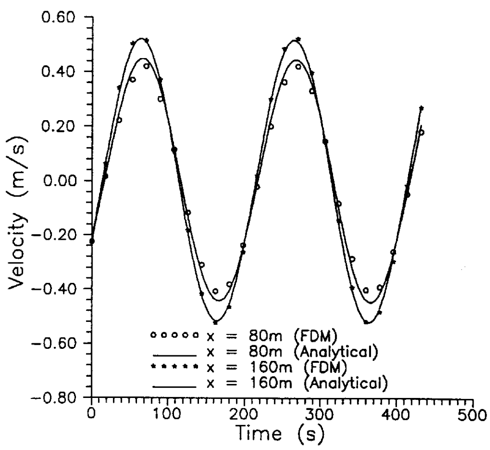

Figure 8. FDM velocity results for channel with quadratic bottom variation, $\tau = 0{\cdot}01\ s^{-1}$

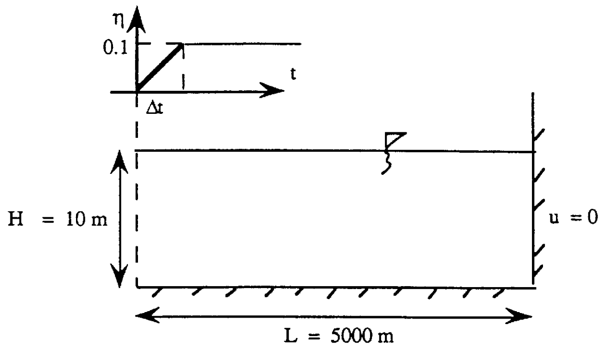

Figure 9. Horizontal, frictionless channel

with $a = L/c$. At the boundary $x = L$ this expression reduces to

$$\eta(L, t_F) = 2\eta(0, t_F - a) - \eta(L, t_F - 2a).$$

The above expression corresponds to a periodic step function of amplitude $h = 10{\cdot}1 \pm 0{\cdot}1$ m and period $T = 2010$ s. Similarly, the exact solution for the discharge at $x = 0$ is $Q = \pm 1$ m^3 s^{-1}.

Consequently, if non-linear terms are neglected, the BEM formulation reproduces the exact solution and no numerical analysis is required. Velocity results were obtained with the finite difference scheme using a discretization of $\Delta x = L/5$ and a time step $\Delta t = 100$ s. The values of the discharge at the upstream end were found to be $Q = \pm 0{\cdot}99753$ m^3 s^{-1}.

If non-linear terms are included, the BEM formulation requires a domain integration. The same discretization and time step as before were used for the numerical solution.

BEM results for the water depth at the downstream end and FDM results for the discharge at the upstream end are shown in Figures 10 and 11 respectively. Both linear and non-linear cases are plotted. It can be concluded from the results that the convective term introduces very small differences in the numerical solutions.

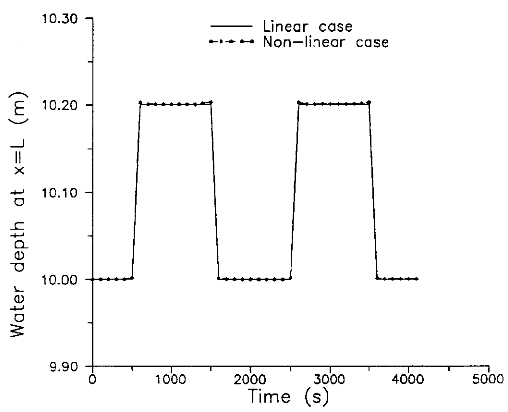

Figure 10. Water depth results for linear and non-linear cases

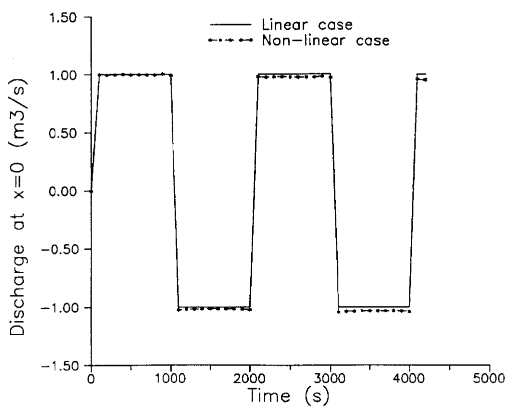

Figure 11. Water discharge results for linear and non-linear cases

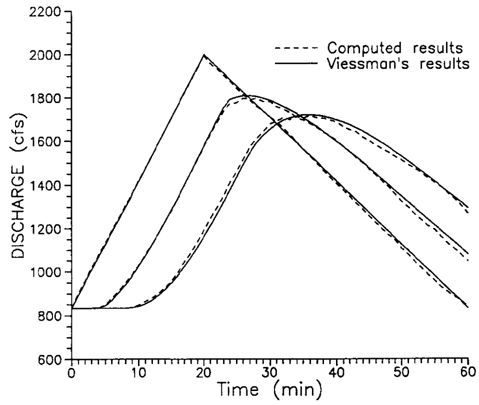

Figure 12. Water discharge at upstream, middle and downstream sections

5.3. *Routing of a triangular hydrograph*

This final test, taken from Reference 16, consists of following the translation of a flood wave down a rectangular channel. The channel is 20 ft wide and 10,560 ft long, carrying a steady uniform discharge of 833·5 $ft^3 s^{-1}$ at 6 ft depth and subject to an upstream flood wave which increases linearly over a period of 20 min and has a peak of 2000 $ft^3 s^{-1}$. This upstream flow then decreases linearly from the peak to the initial discharge in an additional period of 40 min. The channel has a bottom slope of 0·0015 and an estimated Manning coefficient n of 0·02.

In this test the full non-linear equations must be considered, since convective terms are important and the elevation η is of the same order of magnitude as the uniform water depth H. Therefore the iterative scheme previously described is necessary to predict a correct and stable solution.

Since the numerical model employed here deals with the velocity and water depth as dependent variables, the boundary conditions applied in this case are taken from the upstream values of velocities and the downstream values of water depth given in Reference 16.

The explicit method used in Reference 16 utilized $\Delta t = 2$ s and $\Delta x = 528$ ft. Herein the same Δx was retained but a much larger $\Delta t = 30$ s was used. Results obtained with $\theta = 0{\cdot}5$, $\alpha = 0{\cdot}6$ and $\Psi = 0{\cdot}6$ are presented in Figure 12 and show very good agreement with the results given in Reference 16. The small differences in results are attributed to the boundary conditions using velocities and depths instead of discharges.

6. CONCLUSIONS

This paper presented a wave equation formulation for one-dimensional open channel flow. The numerical solution of the wave continuity equation was carried out by the BEM, while the momentum equation was solved using an FDM scheme.

For the BEM formulation the fundamental solution of the wave equation was used and bottom friction, variable bathymetry and non-linear effects were considered through a domain discretization. The corresponding terms were treated as known in each time step by using, in their calculation, values obtained at the previous step. For linear problems an iterative scheme was attempted, but the difference in numerical results was negligible, confirming the efficiency of this time-delayed approximation. Non-linear problems, however, required an iterative scheme which proved to converge quickly.

The FDM results were obtained using an implicit scheme with good accuracy. Several different values of the time-weighting parameters were tested and empirical bounds set.

REFERENCES

1. J. J. Connor and J. D. Wang, 'Finite element modelling of hydrodynamic circulation', in *Numerical Methods in Fluid Dynamics*, Pentech, London, 1974.
2. M. Kawahara, N. Takeuchi and T. Yoshida, 'Two-step explicit finite element method for tsunami wave propagation analysis', *Int. j. numer. methods eng.*, **12**, 331–351 (1978).
3. D. R. Lynch and W. G. Gray, 'A wave equation model for finite element tidal computations', *Comput. Fluids*, **7**, 207–228 (1979).
4. W. J. Mansur and C. A. Brebbia, 'Formulation of the boundary element method for transient problems governed by the scalar wave equation', *Appl. Math. Model.*, **6**, 307–311 (1982).
5. W. J. Mansur and C. A. Brebbia, 'Numerical implementation of the boundary element method for two-dimensional transient scalar wave propagation problems', *Appl. Math. Model.*, **6**, 229–306 (1982).
6. N. Benmansour, D. Ouazar and C. A. Brebbia, 'Boundary element approach to one-dimensional wave equation', in *Computer Methods in Water Resources*, Computational Mechanics Publications, Southampton/Springer, Berlin, 1988.
7. N. Benmansour, L. C. Wrobel, D. Ouazar and C. A. Brebbia, 'Boundary element simulation of shallow water wave equations', in *Computer Methods in Water Resources II*, Computational Mechanics Publications, Southampton/Springer, Berlin, 1991.
8. I. P. E. Kinnmark, *The Shallow Water Wave Equation: Formulation, Analysis and Applications*, LNE Vol. 15, Springer, Berlin, 1986.
9. P. M. Morse and H. Feshbach, *Methods of Theoretical Physics*, McGraw-Hill, New York, 1953.
10. N. Benmansour, 'Boundary element solution to stratified shallow water wave equations', *Ph.D. Thesis*, Wessex Institute of Technology, University of Portsmouth, 1993.
11. I. P. E. Kinnmark and W. G. Gray, 'Time-weighting of the momentum equation in explicit wave equation models of surface water flow', in *Finite Elements in Water Resources IV*, Springer, Berlin, 1982.
12. M. G. G. Foreman, 'An analysis of the wave equation model for finite element tidal computations', *J. Comput. Phys.*, **52**, 290–312 (1983).
13. J. P. Laible, 'A finite element/finite difference wave model for depth varying nearly horizontal flow', *Adv. Water Resources*, **7**, 2–14 (1984).
14. D. R. Lynch and W. G. Gray, 'Analytical solutions for computer flow model testing', *J. Hydraul. Div., ASCE*, **104**, 1409–1428 (1978).
15. U. Meissner, 'An explicit–implicit water-level model for tidal computations of rivers', *Comput. Methods Appl. Mech. Eng.*, **13**, 221–232 (1978).
16. W. Viessman, T. E. Harbaugh and J. W. Knapp, *Introduction to Hydrology*, Intext Educational Publishers, New York, 1972.